Evaluating Computational Methods under the Influence of Noise Terms

OKHUNJON SAYFIDINOV, BAKHTIYOR MARDONOV, AKHMADJON JUMAEV
Mechanical Engineering,
Navoi State University of Mining and Technologies,
Galaba 76v, 210100, Navoi city,
UZBEKISTAN

Abstract: - This paper presents a comprehensive analysis of the Kardar-Parisi-Zhang (KPZ) equation's behavior under various noise conditions and investigates the efficiency of different discretization methods, particularly focusing on the exponential decreasing method and Leapfrog-hopscotch methods. By implementing a series of numerical experiments on a standard computing system, this study evaluates the performance of these numerical approaches in terms of computation speed, accuracy, and stability. Our findings reveal that the Leapfrog-hopscotch method, especially in the absence of noise and under Brownian conditions, exhibits significantly faster computation speeds while maintaining high precision in the simulation of stochastic differential equations (SDEs). Furthermore, the sensitivity of simulation outcomes to changes in both nonlinear (λ) and linear (D) parameters of noise are investigated, which offers new insights into the KPZ equation's response to stochastic influences. These results enhance our understanding of the behavior of complex systems and guide the selection of appropriate numerical methods for practical applications in computational physics, mathematical biology, financial modeling, and stochastic control.

Key-Words: - KPZ equation, noise term, Gaussian noise, pink noise, random noise, discretization method.

Received: April 11, 2024. Revised: September 14, 2024. Accepted: December 19, 2024. Published: March 28, 2025.

1 Introduction

The description of random interface evaluation or surface in a noise environment can be presented by the Kardar-Parisi-Zhang (KPZ) equation, which is a nonlinear stochastic partial differential equation, [1]. By a generalization of the Edwards-Wilkinson (EW) equation, we obtain the KPZ equation [2], which is a linear stochastic equation for surface growth. Many researchers paid attention to the KPZ equation in mathematics and physics due to its rich and universal behavior [3], as well as its connections to various phenomena such as directed polymers [4], random matrices [5], turbulence [6], and fluid dynamics [7].

The most important point of the KPZ equation is the existence of a noise component [8], which presents the random oscillations of the contact or surface [9]. Considering the nature and strength of the noise, the KPZ equation can show various scaling features and asymptotic behavior. Particularly, existence of a noise component, has the potential to influence the roughness exponent, which measures how uneven the contact or surface is, as well as the growth exponent, by measuring how quickly it increases. These exponents are connected by a scaling relation that depends on the system's dimension, [10].

In this paper, we will compare the discretized KPZ equation in the presence of numerous noise components. In detail, we study the performance of the Heun [11] and Leapfrog-Hopscotch [12] methods on partial differential equations (PDEs) including various forms of noise, such as white noise [13], Gaussian noise [14], random noise [15], Brownian noise [16] and pink noise [17]. Various statistical features of the underlying stochastic processes can be obtained by these noise factors and have unique consequences on the system dynamics.

In order to solve ordinary differential equations (ODEs) and SDEs, we used a numerical approach, such as the Heun method [11] mostly known as the modified Euler method, [18]. The method is a second-order accurate technique that uses a predictor-corrector strategy to increase accuracy while being as simple as the Euler method. On the other hand, the Leapfrog HopScotch method [12] is a recently created discretization scheme that is built for SDEs. This method provides benefits in terms of stability and computing efficiency.

We will simulate and concentrate on a full comparison of numerical experiments on a laptop computer (ASUS, Taiwan) with a 2.6 GHz Intel i7-10750H CPU, 8.0 GB RAM with the MATLAB R2022b software (The MathWorks, Inc., Portola

Valley, CA, USA) with various noise terms. All discretization method's performances will be evaluated in terms of computation speed, accuracy, and stability. Our investigation will be on the sensitivity of the results to adjustments in the parameters of the noise terms such as Gaussian, white, brown, pink, and random noises. Furthermore, in order to further investigate, we will perform parameter analysis of the nonlinear (λ) and linear terms (D). B

Our research intends to contribute to a better understanding of the behavior of different discretization methods with different parameters of linear and nonlinear terms in the setting of SDEs with varying noise components, by offering insights that can help guide the selection of appropriate numerical approaches for specific applications. The conclusions of this study have ramifications for computational physics, mathematical biology, financial modeling, and stochastic control.

2 KPZ Equation and Methods

The KPZ equation presents the local growth rate of a profile $h(x,t)$ at a substrate position x and time t [1]:

$$\frac{\partial h(x,t)}{\partial t} = D\nabla^2 h + \frac{\lambda}{2}(\nabla h)^2 + k(x,t), \quad (1)$$

where variations in parameters D (diffusion coefficient) and λ (nonlinear parameter). In this study, we will address the KPZ equation and we will examine the impact of two distinct noise terms, denoted as $k(x,t)$ specifically, Gaussian noise, Brownian noise, pink noise, and random noise. The detailed analysis of these noise terms will be elaborated upon in section 3.3.

In our research, we continue our previous research results verification [19] which applied the traditional discretized method and new numerical methods to the time-integration of the spatially discretized KPZ equation. However, we will present brief information about verification using an analyticalanalytical solution and comparison result of the Gaussian noise effect for parameters of diffusion coefficient (D) and nonlinear parameter (λ).

2.1 The Adaptation of the Forward Time-Centered Space (FTCS) Scheme

In their paper [20], researchers proposed a method to incorporate spatial derivatives into the right-hand side of the KPZ equation (1). This approach involved discretizing the equation using standard forward-backward differences on a cubic grid with a lattice constant Δx, commonly referred to as the forward time centered space (FTCS) scheme, [21].

$$h_i^{n+1} = h_i^n + r(h_{i+1}^n + h_{i-1}^n - 2h_i^n) + \mu(h_{i+1}^n - h_{i-1}^n)^2 + \Delta t\, k(x,t), \quad (2)$$

where Δt is the step size and $t_{i+1} = t_i + \Delta t$, $r = \frac{\upsilon \Delta t}{\Delta x^2}$ and $\mu = \frac{\lambda \Delta t}{8\Delta x^2}$ are the appropriate mesh ratios. In the computational process delineated for evaluating the right-hand side of Equation (2), an iterative procedure is employed, traversing each node within the system through a `for` loop. This approach necessitates the exclusive use of a singular array designated for the variable (h), comprising a number of elements equivalent to the node count. The computation of (h_{i+1}^n) requires the preceding value (h_{i-1}^n), compelling the introduction of a provisional auxiliary array to retain these computed values. Subsequently, only upon the iterative loop's completion are the updated values (h_{i+1}^n) transferred to the primary array. This methodological outline explicates the rationale behind the potential for optimization of this ostensibly straightforward algorithm, a hypothesis that will be substantiated through further analysis in the ensuing sections.

2.2 Leapfrog-hopscotch Method

The innovative leapfrog-hopscotch (LH) framework was initially introduced and delineated in recently published paper, [12]. This methodology draws parallels to the foundational odd-even hopscotch (OEH) algorithm, a concept that emerged five decades prior through the seminal works [22] and [23]. The essence of this approach necessitates the segregation of the computational grid into two distinct subsets of nodes, classified as odd and even (illustrated as light blue and dark red dots in Figure 1), ensuring that each odd node is surrounded by even nodes and vice versa. The computational process commences with the application of a reduced time step for the odd nodes, leveraging the initial values, as depicted by green arrows in Figure 1. Subsequently, the algorithm alternates between full time step calculations for even and odd nodes (represented by light blue and dark red arrows), culminating in a final time step where the size is similarly reduced for the odd nodes, indicated by purple arrows.

$$h_i^{n+1} = \frac{2h_i^n + r(h_{i-1}^{recent} + h_{i+1}^{recent})}{2(1+r)} + \frac{\mu\,(h_{i-1}^{recent} - h_{i+1}^{recent})^2 + k\left(x, t^n + \frac{\Delta t}{2}\right)\Delta t}{2(1+r)} \quad (3)$$

This procedure employs the most recent h values of the neighboring nodes (h_{i+1}^{recent}), thereby categorizing the method as explicit. Our detailed examination of this LH structure, specifically applied to the diffusion equation, was presented in [12]. Through extensive numerical analysis, we determined that the UPFD formula exhibits optimal performance at the zeroth time step, while the $\theta = \frac{1}{2}$ formula proves efficacious in successive steps. Consequently, this tailored approach, incorporating both the LH time-space structure and the specified formulas, is hereby designated as "the LH method." Our comprehensive analysis in [12] analytically and numerically affirmed the unconditional stability of this method when applied to the diffusion equation, also noting its comparative accuracy to Heun's method. As such, we proposed the adaptation of the LH method [19] for application to the KPZ equation.

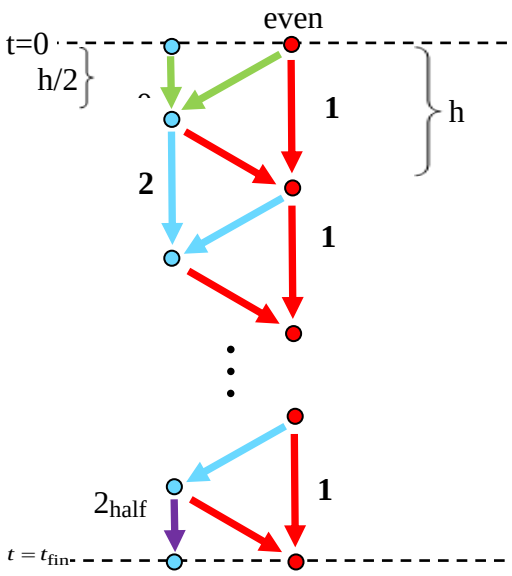

Fig. 1: The new leapfrog-hopscotch structure

In the context of the one-dimensional KPZ equation, as detailed in references [24], [25], we communicate the revised valuation of the h variable throughout the initial iteration phase.:
and at all other steps (denoted by 1 and 2 in Figure 1):

$$h_i^{n+1} = \frac{(1-r)h_i^n + r\left(h_{i-1}^{recent} + h_{i+1}^{recent}\right)}{1+r} + \\ + \frac{\mu\left(h_{i-1}^{recent} - h_{i+1}^{recent}\right)^2 + k(x, t^n + \Delta t/2)\Delta t}{1+r} \quad (4)$$

excluding the final iteration with a half timestep, equation (7) requires the substitution $\Delta t \to \frac{\Delta t}{2}, r \to \frac{r}{2}, \mu \to \frac{\mu}{2}$. Setting μ and k to zero returns the LH technique to its original form, which was designed for the diffusion equation. The intrinsic time-space layout of the LH technique eliminates the need for auxiliary arrays to hold intermediate h values, decreasing memory requirements. As a result, this property makes the LH approach somewhat more efficient in terms of computing speed when compared to the core FTCS method. Taking into account this information, we have done verification using an analitical solution and found out that the stable and accurate method is LH approach, [19].

2.3 Exponential Decreasing Method

In the computational simulations conducted, the discretized form of the temporally correlated Kardar-Parisi-Zhang (KPZ) equation is found to exhibit numerical instabilities within the effective lambda parameter regime, as delineated in [8]. This instability precludes the observation of system evolution in scenarios characterized by singular growth phenomena extending beyond the established temporal bounds. To circumvent these numerical instabilities, the study adopts a modification strategy predicated on the replacement of the nonlinear term with an exponentially decaying function. This proposed approach [15], demonstrates efficacy in stabilizing the numerical simulations and allowing for continued observation of the system's evolution within the specified parameter space.

$$f(x) \equiv \frac{1 - e^{-cx}}{c}, \quad (5)$$

where, the variable c is introduced as an adjustable parameter. Previous research indicated by reference [15] suggests that the multiscaling phenomena observed within the context of growth models exhibit a non-universal and transient nature. This characteristic prevails across all magnitudes of the control parameter c, contingent upon c being sufficiently large to sustain a power-law scaling in the surface width W. Under these conditions, the scaling exponents are well-defined. Given the parameter c is set to unity, complexities arise in determining the values of the coefficient λ associated with the nonlinear term. Consequently, the ensuing form of the modified temporally correlated Kardar-Parisi-Zhang (KPZ) equation in a (1+1)-dimensional framework is delineated as follows:

$$h_i^{n+1} = h_i^n + v\frac{\Delta t}{(\Delta x)^2}[h_{i+1}^n - 2h_i^n + h_{i-1}^n] \\ + \Delta t \frac{\lambda}{2c}\left[1 - e^{-c\left[\frac{h_{i+1}^n - h_{i-1}^n}{2\Delta x}\right]^2}\right] + \eta_i^n, \quad (6)$$

$$\eta_i^n = \sqrt{\frac{2D}{\Delta x^d}}\sqrt{12\Delta t}\cdot R(t).$$

3 Numerical Solution

Initially, we have numerically simulated only Gaussian noise to observe the dynamics of a system with varying intensities denoted by parameter D. The system is characterized by parameters $\lambda = 0.01, c = 1.18, a = 0.1, L = 64,$ and $\Delta t = 10^{-5}$, which govern the behavior of the system over a spatial domain and a discrete time-step.

The Figure 2 appears to depict a succession of waveforms, each showing a distinct value of the noise intensity D. As D grows, the amplitude of the waveforms shows different fluctuations, indicating that noise has an impact on the system's stability and propagation properties.

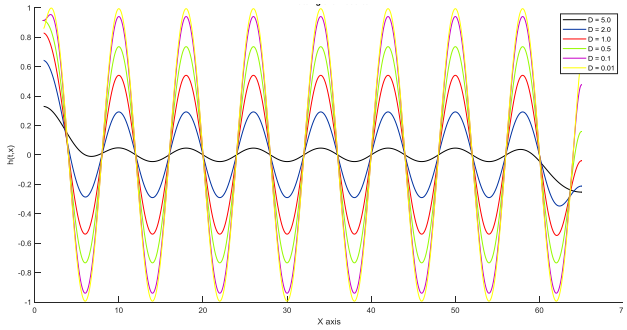

Fig. 2: Numerical simulation of Gaussian noise for different D while $\lambda = 0.01$, $c = 1.18$, $a = 0.1$, L=64, and $\Delta t = 10^{-5}$

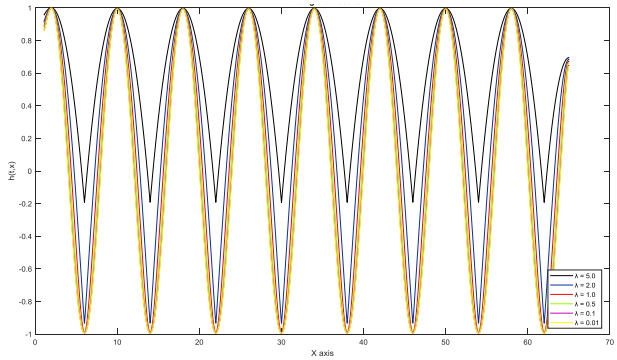

Fig. 3: Numerical simulation of Gaussian noise effect for different value of λ while $D = 0.01$, $c = 1.18$, $a = 0.1$, L=64, $\Delta t = 10^{-5}$

The simulation results presented in the Figure 3 illustrate the influence of the parameter of linear term on a system subjected to Gaussian noise which varies between $D = 0.01$ and 5.0. Other parameters remain fixed with $\lambda = 0.01, c = 1.18, a = 0.1, L = 64$, and $\Delta t = 10^{-5}$. The parameter λ is typically associated with a rate or a scale in the system, and the simulations demonstrate how its variation affects the system's behavior. The increase of D decrease the surface hight $h(t,x)$ that makes the surface smoother.

3.1 The Noise Terms

One can see in Figure 3 that the curves are indistinguishable, which means that each method is accurate. The (global) numerical difference is the absolute difference of the numerical solutions h_i^{num} produced by the examined methods at final time t_{fin} for KPZ equation: the FTCS scheme, the Heun method, and the LH method for 10^{-5} and 10^{-4} time step size. For brevity, we denote this latter case, the LH method with 10^{-4} time step size as LH*.

In order to find the individual difference between the nodes or cells, we calculate the maximum and average differences in following ways:

$$\begin{aligned} D_i^{FTCS,LH} &= \left|h_i^{FTCS} - h_i^{LH}\right|, \\ D_i^{FTCS,DG} &= \left|h_i^{FTCS} - h_i^{DG}\right|, \\ D_i^{DG,LH} &= \left|h_i^{DG} - h_i^{LH}\right| \end{aligned} \tag{7}$$

Average differences (L_1 errors)

$$\begin{aligned} L_1^{FTCS,LH} &= \sum_i \frac{D_i^{FTCS,LH}}{Nx}, \\ L_1^{LH,DG*} &= \textstyle\sum_i \frac{D_i^{LH,LH*}}{Nx}, \text{ etc} \end{aligned} \tag{8}$$

Maximum differences (L_∞ errors)

$$\begin{aligned} L_\infty^{FTCS,LH} &= \max_i\{D_i^{FTCS,LH}\}, \\ L_\infty^{LH,DG} &= \max_i\{D_i^{LH,DG}\}, \quad \text{etc} \end{aligned} \tag{9}$$

3.2 Investigating the Impact of Varied Noise Terms on System Dynamics: A Comprehensive Analysis

In order to establish a comparison with prior studies conducted in a one-dimensional framework [17], [26], we examine a range of analytic noise terms to determine their capacity to yield analytic solutions. This examination is critical for validating the consistency of the results across different dimensional configurations and for extending the applicability of the findings derived from our previous investigations, [19].

$\varepsilon = a\omega_n$ colored noises $n = -2. - 1$ are brown and pink, respectivelly

$\varepsilon = ae^{-b\omega^2}$ Gaussian noise

$R(t) = a + (b - a)\cdot rand(\Delta t, \Delta x)$, where $rand(t1, x1)$ returns a t1 by x1 array of random numbers where $t1, \ldots, x1$ indicate the size of each dimension.

3.3 Comparison of Different Noise Terms for Certain Values of D and λ

In an experiment, the numerical values of D and λ depend on the specific system being studied. Numerous studies have been carried out on the KPZ equation in different physical systems [27], [28] and the values of these parameters can vary widely depending on the experimental conditions .

Previous investigations of the growth mechanisms of a component are based on the Kardar-Parisi-Zhang universality class. The scaling exponents of metals in previous studies were found to be between 0.22 and 0.56. Studies using thermal evaporation sources gave consistent scaling exponents of around 0.25 for iron [29] and silver [30], [31]. In the present study, a scaling exponent of 0.3 was found, which coincides with the scaling exponents of gold and molybdenum films deposited by sputtering. However, these values are greater than 0.25, predicted by the KPZ equation for the 2+1 system, [30], [31].

Other studies have found different values of D and λ in different systems. For example, in a study of bacterial colonies, the roughness exponent was found to be around 0.5, while the growth exponent was around 1.25. In an electrodeposition study, the roughness exponent was found to be around 0.8, while the growth exponent was around 1.5, [32].

In general, the values of D and λ in real experiments depend on the specific physical system studied and the experimental conditions. The KPZ equation has been proven to be a useful tool for describing the behavior of growing surfaces in a wide range of systems, [33], [34].

The Figure 4 presents the maximum difference error (9) as a function of the control parameter λ, investigated over a range of values including $0.01, 0.1, 0.5, 1, 2,$ and 5. The analysis delineates the behavior under different noise conditions compared to the noise-free scenario. In the absence of noise, denoted by the red line, the error remains relatively constant, exhibiting minimal variation across the spectrum of lambda values. In contrast, the introduction of Gaussian noise, illustrated by the blue line, indicates a gradual increase in error with rising lambda values, suggesting a noise-dependent deviation from the noise-free case. The Brownian noise, depicted by the black line, and pink noise, indicated by the pink line, both demonstrate intermediate behavior with a modest increment in error as lambda increases, albeit at a lower rate than the Gaussian noise. Notably, the yellow line representing random noise shows a marked increase, particularly beyond the lambda value of 1, signifying a pronounced sensitivity to this form of noise. The data exhibits a sharp upward trend in the error for lambda values greater than 1, reaching a peak at lambda equal to 5 for the random noise scenario. This pronounced error escalation in the presence of random noise underscores the significant impact of stochastic fluctuations on the system's dynamics, particularly at higher values of the control parameter lambda.

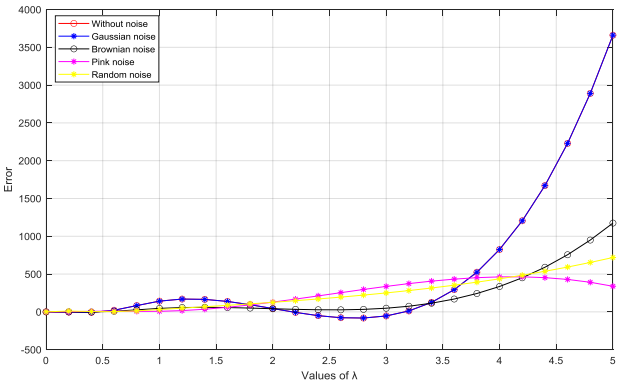

Fig. 4: Calculation of Error to different values of L with various noise terms

The graph depicts the variation of the maximum difference error (9) as a function of the linear term D, evaluated across a discrete set of values: 0.01, 0.1, 0.5, 1, 2, and 5. The investigation was conducted under multiple noise conditions to ascertain the influence of stochastic factors on error magnitude.

In Figure 5 the red line, representing the system without noise, maintains a relatively stable error value across lower D values, with a notable peak at $D = 1$, before decreasing as D increases further. The Gaussian noise, shown in blue, reveals a consistently moderate error across the D values, with a slight increase peaking around $D = 0.5$ before a gradual descent. The black line, indicating Brownian noise, and the pink line, denoting pink noise, both display a non-monotonic relationship with the linear term D, with a prominent trough at $D = 1$, suggesting a minimum error at this point, followed by an increase in error at higher values of D.

The yellow line, illustrating random noise, demonstrates a starkly contrasting behavior, characterized by a significant descent into negative error values, reaching a nadir at $D = 1$, and subsequently inverting this trend beyond $D = 1$. This pronounced dip into negative error values indicates an inverse relationship between the linear term D and the system's stability under random noise conditions, up to the point of $D = 1$, after which the error ascends with increasing values of D.

These results show that the nature of noise within a system can significantly affect the error dynamics, especially in relation to the value of the linear term D. The random noise, in particular, introduces a distinct pattern of error behavior, underscoring the critical role of stochastic influences in determining system performance.

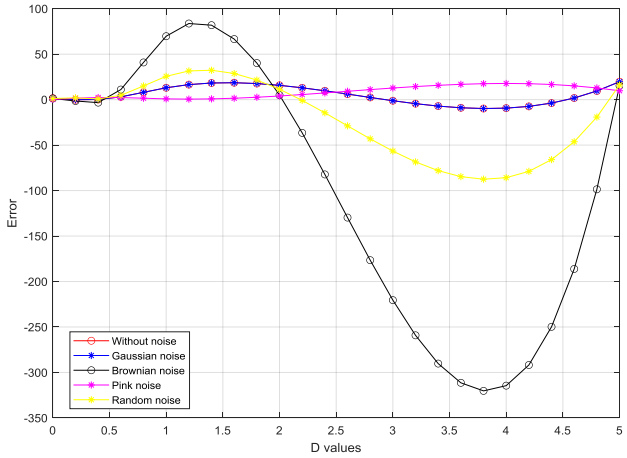

Fig. 5: Calculation of Error to different values of D with various noise terms

Figure 6 represents the outcomes of an empirical investigation into the computation time required by the Leapfrog-hopscotch method, under the influence of various noise terms. The computation time t has been measured across an array of values for the non-linear term λ, specifically 0.01, 0.1, 0.5, 1, 2, and 5.

The data reveals that in the absence of any noise, indicated by the red line, the simulation time remains relatively invariant regardless of the lambda value, suggesting that the noise-free Leapfrog-hopscotch method's performance is robust to changes in the non-linearity parameter.

Upon the introduction of Gaussian noise, represented by the blue line, there is a discernible oscillation in simulation time, with peaks at lambda values of 0.1 and 5, and a notable valley at lambda equals 1. This indicates that Gaussian perturbations can lead to an increased computational demand at certain levels of non-linearity.

For Brownian noise, marked by the black line, the simulation time exhibits a significant peak at lambda equals 0.5, followed by a decrease as lambda increases, eventually stabilizing. This pattern suggests a complex interplay between the non-linear dynamics and the memory-dependent characteristics of Brownian motion.

The system under the influence of pink noise, shown in pink, demonstrates a steady increase in simulation time up to lambda equals 2, after which it plateaus. This suggests a threshold in the noise's effect on computation time.

Contrastingly, random noise, depicted by the yellow line, leads to a fluctuating computation time with the largest variability across the studied range, especially notable for lambda values greater than 1, where the computation time sharply rises, peaking at lambda equals 5.

These results underscore the critical influence of stochastic variations on the computational efficiency of numerical methods. Specifically, they demonstrate that the nature of noise can significantly affect the simulation time required by the Leapfrog-hopscotch algorithm, which is a crucial consideration for computational modeling practices.

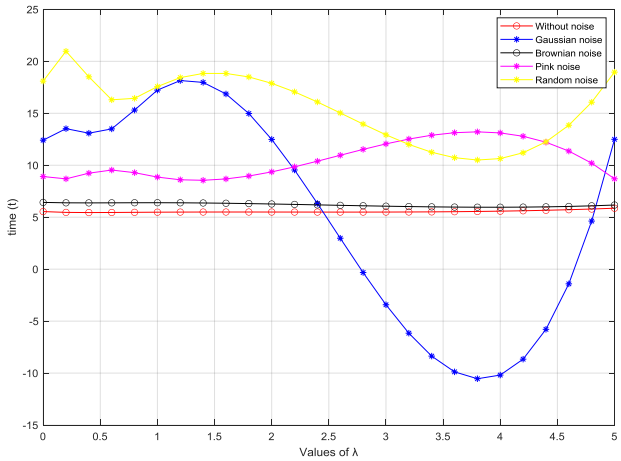

Fig. 6: Assessment of simulation time across different noise terms using the Leapfrog-hopscotch method

The investigation assesses the computational duration required for simulations applying the Leapfrog-hopscotch method across varying values of the linear term D. The values of D under consideration are 0.01, 0.1, 0.5, 1, 2, and 5. Simulation time is a critical metric, indicative of algorithm efficiency under different stochastic conditions.

In Figure 7 the baseline case, denoted by the red line, where no noise term is included, demonstrates a consistent simulation time across all values of D, establishing a reference point for noise-impacted scenarios. The simulation time for the Gaussian noise, represented by the blue line, initially displays a significant decrease at lower values of D, stabilizing to a relatively invariant duration as D increases. This suggests that Gaussian noise has a diminishing impact on simulation time beyond a certain threshold of D.

In contrast, Brownian noise, represented by the black line, shows an insignificant decrease in simulation time with increasing D, maintaining a moderate and relatively stable duration throughout the range. The pink noise, shown in pink, exhibits a more nuanced pattern, with simulation time increasing until $D = 1$ before decreasing; this could indicate an optimal efficiency point at $D = 1$ for this type of noise. It can be seen that the most significant pattern is observed with random noise, represented by the yellow line. Here, simulation time increases with D until reaching a plateau at approximately $D = 1$, after which it remains relatively steady. The plateau reached indicates that there may be a nonlinear response of the simulation time to the linear D term only in the presence of random noise, indicating a possible dependence on the type of noise and the simulation method used.

To summarize, all these results may mean that the D term is a linear factor that interacts with each noise term in its own unique way, thus affecting the simulation time taken by the Leapfrog-hopscotch method. The Gaussian and Brownian noise factors appear to contribute less and less to the simulation time as D increases, while pink noise appears to be most effective at $D = 1$. On the other hand, random noise increases the simulation time, although it eventually reaches a plateau, suggesting more complex boundaries that need to be optimized in terms of computational resources used.

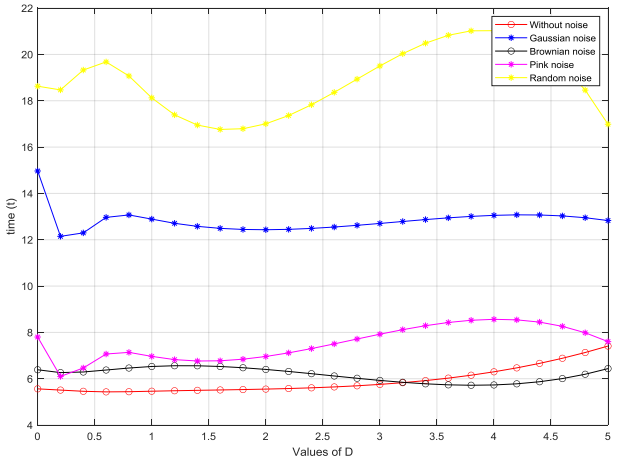

Fig. 7: Simulation time analysis using the Leapfrog-hopscotch method across different noise terms and D values

4 Conclusion

The study has shown a new frontier in understanding and connection between noise terms and discretization methods which are FTCS, DG, Leapfrog-hopscotch on the KPZ equation at nonlinear λ and linear parameters D. From the computations we have performed, we can see that multiple noise components such as Gaussian, Brownian, pink and even random noise significantly affect the stability and error function metrics of the system. It is also interesting that the presence of Gaussian and the absence of noise affects the behavior of the system, especially at higher values of λ. Their modeling of noise characteristics is crucial in computation.

In addition, this study reveals new details about computational efficiency, showing that the Leapfrog-hopscotch method outperforms all other methods in solving problems with different noise levels and a range of parameters in terms of speed and accuracy. Modeling with Brownian noise and modeling without noise proved to be the fastest. With Brownian noise and without noise, the speed of computation was the fastest with accuracy, which is a huge step in the numerical modeling of stochastic differential equations. The fastest computation with added noise was achieved without other methods. Such results point to the possibility of developing algorithms that are much more sophisticated and perform better in fields ranging from physics to financial modeling, where systems behave in complex ways. This research greatly improves the understanding of the best approaches to numerical methods that can be used to model real-world situations filled with noise.

Declaration of Generative AI and AI-assisted Technologies in the Writing Process

During the preparation of this work the authors used ChatGPT in order to improve the readability and language of the manuscript. After using this tool/service, the authors reviewed and edited the content as needed and take full responsibility for the content of the publication.

References:

[1] M. Kardar, G. Parisi, and Y.-C. Zhang, ‘Dynamic Scaling of Growing Interfaces’, *Phys. Rev. Lett.*, vol. 56, no. 9, pp. 889–892, Mar. 1986, doi: 10.1103/PhysRevLett.56.889.

[2] S. F. Edwards, ‘DR Wilkinson Proc’, in *R. Soc. London, Ser. A*, 1982, p. 17, doi: 10.1098/rspa.1982.0056.

[3] D. Muraca, L. A. Braunstein, and R. C. Buceta, ‘Universal behavior of the coefficients of the continuous equation in competitive growth models’, *Physical Review E*, vol. 69, no. 6, p. 065103, 2004.

[4] P. Le Doussal and P. Calabrese, 'The KPZ equation with flat initial condition and the directed polymer with one free end', *J. Stat. Mech.*, vol. 2012, no. 06, p. P06001, Jun. 2012, doi: 10.1088/1742-5468/2012/06/P06001.

[5] H. Spohn, 'Exact solutions for KPZ-type growth processes, random matrices, and equilibrium shapes of crystals', *Physica A: Statistical Mechanics and its Applications*, vol. 369, no. 1, pp. 71–99, Sep. 2006, doi: 10.1016/j.physa.2006.04.006.

[6] M. K. Verma, 'Intermittency exponents and energy spectrum of the Burgers and KPZ equations with correlated noise', *Physica A: Statistical Mechanics and its Applications*, vol. 277, no. 3–4, pp. 359–388, Mar. 2000, doi: 10.1016/S0378-4371(99)00544-0.

[7] I. V. Protopopov, R. Samanta, A. D. Mirlin, and D. B. Gutman, 'Anomalous Hydrodynamics in a One-Dimensional Electronic Fluid', *Phys. Rev. Lett.*, vol. 126, no. 25, p. 256801, Jun. 2021, doi: 10.1103/PhysRevLett.126.256801.

[8] T. Song and H. Xia, Numerically stable neural network for simulating Kardar-Parisi-Zhang growth in the presence of uncorrelated and correlated noises. 2023. *arXiv preprint arXiv:2306.06952*, doi: 10.48550/ARXIV.2306.06952.

[9] F. D. A. Aarão Reis, 'Scaling in the crossover from random to correlated growth', *Phys. Rev. E*, vol. 73, no. 2, p. 021605, Feb. 2006, doi: 10.1103/PhysRevE.73.021605.

[10] J. Magnen and J. Unterberger, 'The Scaling Limit of the KPZ Equation in Space Dimension 3 and Higher', *J Stat Phys*, vol. 171, no. 4, pp. 543–598, May 2018, doi: 10.1007/s10955-018-2014-0.

[11] Ronveaux, A. and Arscott, F.M. eds., 1995. *Heun's differential equations*. Clarendon Press. ISBN: 9780198596950.

[12] Á. Nagy, I. Omle, H. Kareem, E. Kovács, I. F. Barna, and G. Bognar, 'Stable, Explicit, Leapfrog-Hopscotch Algorithms for the Diffusion Equation', *Computation*, vol. 9, no. 8, p. 92, Aug. 2021, doi: 10.3390/computation9080092.

[13] M. Hoshino, 'KPZ equation with fractional derivatives of white noise', *Stoch PDE: Anal Comp*, vol. 4, no. 4, pp. 827–890, Dec. 2016, doi: 10.1007/s40072-016-0078-x.

[14] M. Hairer, 'Solving the KPZ equation', *Annals of Mathematics*, vol. 178, no. 2, pp. 559–664, 2013.

[15] C. Dasgupta, J. M. Kim, M. Dutta, and S. Das Sarma, 'Instability, intermittency, and multiscaling in discrete growth models of kinetic roughening', *Phys. Rev. E*, vol. 55, no. 3, pp. 2235–2254, Mar. 1997, doi: 10.1103/PhysRevE.55.2235.

[16] J. Calvert, A. Hammond, and M. Hegde, 'Brownian structure in the KPZ fixed point', 2019, doi: 10.48550/ARXIV.1912.00992, 2019 Dec 2.

[17] I. F. Barna, G. Bognár, M. Guedda, L. Mátyás, and K. Hriczó, 'Analytic self-similar solutions of the Kardar-Parisi-Zhang interface growing equation with various noise terms', *Mathematical Modelling and Analysis*, vol. 25, no. 2, pp. 241–256, Mar. 2020, doi: 10.3846/mma.2020.10459.

[18] A. H. Workie, 'Small Modification on Modified Euler Method for Solving Initial Value Problems', *Abstract and Applied Analysis*, vol. 2021, pp. 1–5, Jul. 2021, doi: 10.1155/2021/9951815.

[19] O. Sayfidinov, G. Bognár, and E. Kovács, 'Solution of the 1D KPZ Equation by Explicit Methods', *Symmetry*, vol. 14, no. 4, p. 699, Mar. 2022, doi: 10.3390/sym14040699.

[20] K. Moser, J. Kertész, and D. E. Wolf, 'Numerical solution of the Kardar-Parisi-Zhang equation in one, two and three dimensions', *Physica A: Statistical Mechanics and its Applications*, vol. 178, no. 2, pp. 215–226, 1991.

[21] G. W. Recktenwald 'Finite-difference approximations to the heat equation'. Mechanical Engineering. 2004 Jan 21;10(01).

[22] P. Gordon, 'Nonsymmetric Difference Equations', *Journal of the Society for Industrial and Applied Mathematics*, vol. 13, no. 3, pp. 667–673, Sep. 1965, doi: 10.1137/0113044.

[23] A. R. Gourlay, 'Hopscotch: a Fast Second-order Partial Differential Equation Solver', *IMA J Appl Math*, vol. 6, no. 4, pp. 375–390, 1970, doi: 10.1093/imamat/6.4.375.

[24] Á. Nagy, M. Saleh, I. Omle, H. Kareem, and E. Kovács, 'New Stable, Explicit, Shifted-Hopscotch Algorithms for the Heat Equation', *MCA*, vol. 26, no. 3, p. 61, Aug. 2021, doi: 10.3390/mca26030061.

[25] M. Saleh and E. Kovács, 'New Explicit Asymmetric Hopscotch Methods for the Heat Conduction Equation', in *The 1st International Electronic Conference on Algorithms*, MDPI, Sep. 2021, p. 22. doi: 10.3390/IOCA2021-10902.

[26] I. F. Barna, G. Bognár, M. Guedda, K. Hriczó, and L. Mátyás, 'Analytic traveling-wave solutions of the Kardar-Parisi-Zhang interface growing equation with different kind of noise terms', vol. 333, 2020, pp. 239–253. doi: 10.1007/978-3-030-56323-3_19.

[27] G. Ódor, B. Liedke, and K.-H. Heinig, 'Directed d -mer diffusion describing the Kardar-Parisi-Zhang-type surface growth', *Phys. Rev. E*, vol. 81, no. 3, p. 031112, Mar. 2010, doi: 10.1103/PhysRevE.81.031112.

[28] R. Van Roij, P. Bolhuis, B. Mulder, and D. Frenkel, 'Transverse interlayer order in lyotropic smectic liquid crystals', *Phys. Rev. E*, vol. 52, no. 2, pp. R1277–R1280, Aug. 1995, doi: 10.1103/PhysRevE.52.R1277.

[29] J. Chevrier, V. L. Thanh, R. Buys, and J. Derrien, 'A RHEED Study of Epitaxial Growth of Iron on a Silicon Surface: Experimental Evidence for Kinetic Roughening', *Europhys. Lett.*, vol. 16, no. 8, pp. 737–742, Oct. 1991, doi: 10.1209/0295-5075/16/8/006.

[30] Y.-L. He, H.-N. Yang, T.-M. Lu, and G.-C. Wang, 'Measurements of dynamic scaling from epitaxial growth front: Fe film on Fe(001)', *Phys. Rev. Lett.*, vol. 69, no. 26, pp. 3770–3773, Dec. 1992, doi: 10.1103/PhysRevLett.69.3770.

[31] P. Hale *S. Turgeon, P. Horny, F. Lewis, N. Brack, Van G. Riessen, P. Pigram, and D. Mantovani,* 'X-ray Photoelectron Emission Microscopy and Time-of-Flight Secondary Ion Mass Spectrometry Analysis of Ultrathin Fluoropolymer Coatings for Stent Applications', *Langmuir*, vol. 24, no. 15, pp. 7897–7905, Aug. 2008, doi: 10.1021/la8002788.

[32] E. Ben-Jacob, O. Schochet, A. Tenenbaum, I. Cohen, A. Czirók, and T. Vicsek, 'Generic modelling of cooperative growth patterns in bacterial colonies', *Nature*, vol. 368, no. 6466, pp. 46–49, Mar. 1994, doi: 10.1038/368046a0.

[33] Muminov, R., Yakhshiev, S., Ravshanov, J., Oripov, Z., Juraev, N., & Maxmudova, M. (2024). Development of technical solutions for modernization of the rotary feed mechanism of a quarry drilling rig. In *E3S Web of Conferences* (Vol. 486, p. 05007). EDP Sciences.

[34] Mardonov, B., Oripov, Z., Muminov, R., Ravshanov, J. and Jo'rayev, N., 2023. Effect of dispersed particles of aluminum oxide on the degree of defects of the crystalline structure of the chromium coating. In *E3S Web of Conferences* (Vol. 417, p. 06001). EDP Sciences.

Contribution of Individual Authors to the Creation of a Scientific Article (Ghostwriting Policy)

- Okhunjon Sayfidinov carried out the simulation and Akhmadjon Jumaev did the optimization.
- Bakhtiyor Mardonov has supervised and executed the experiments of Section 3.

Sources of Funding for Research Presented in a Scientific Article or Scientific Article Itself

There is not any Sources of Funding.

Conflict of Interest

The authors declare no conflict of interest.